

# Optomechanical damping of a nanomembrane inside an optical ring cavity

Arzu Yilmaz, Simon Schuster, Philip Wolf, Dag Schmidt, Max Eisele, Claus Zimmermann, Sebastian Slama

*Physikalisches Institut and Center for Collective Quantum Phenomena in LISA+,  
Eberhard Karls Universität Tübingen, Auf der Morgenstelle 14, D-72076 Tübingen, Germany*

(Dated: May 14, 2019)

We experimentally and theoretically investigate mechanical nanooscillators coupled to the light in an optical ring resonator made of dielectric mirrors. We identify an optomechanical damping mechanism that is fundamentally different to the well known cooling in standing wave cavities. While, in a standing wave cavity the mechanical oscillation shifts the resonance frequency of the cavity in a ring resonator the frequency does not change. Instead the position of the nodes is shifted with the mechanical excursion. We derive the damping rates and test the results experimentally with a silicon-nitride nanomembrane. It turns out that scattering from small imperfections of the dielectric mirror coatings has to be taken into account to explain the value of the measured damping rate. We extend our theoretical model and regard a second reflector in the cavity that captures the effects of mirror back scattering. This model can be used to also describe the situation of two membranes that both interact with the cavity fields. This may be interesting for future work on synchronization of distant oscillators that are coupled by intracavity light fields.

PACS numbers:

## I. INTRODUCTION

Optomechanical forces acting on micro- and nanomechanical systems have been intensively investigated due to their fundamental aspects in quantum mechanics of macroscopic bodies and because of possible applications in quantum metrology and hybrid quantum systems [1]. Important progress has been achieved during the last years in cooling mechanical oscillators to their vibrational ground state [2, 3]. The underlying damping mechanism involves the coupling of a mechanical mode of the oscillator with an optical mode that is typically provided by the light field inside a standing wave cavity. Complementary setups have been realized: cavities with an oscillating end mirror [4, 5], membrane-in-the-middle (MIM) cavities [6, 7], and evanescent-wave resonators [8]. In all of these situations the optomechanical interaction is based on the shift of the cavity mode resonance frequency  $\omega_c(x)$  when the mechanical oscillator is displaced by  $x$ . This is quantified in the parameter  $G = \frac{d\omega_c}{dx}$  [1].

For a membrane in a high finesse optical ring resonator made from standard dielectric mirrors the optomechanical damping is fundamentally different. An empty ring cavity supports two degenerate modes formed by two counter circulating travelling waves. As long as there is no coupling between the waves their relative phases are independent. A membrane inside the cavity scatters light between the two modes and locks their phases. This mode coupling also lifts the degeneracy which leads to a line splitting in the cavity spectrum. The two new eigenmodes are standing waves formed by orthogonal superpositions of the circulating waves. The crucial point now is that the nodes of these standing waves are locked to the position of the membrane. If the membrane is displaced in the cavity the standing waves are displaced by the same amount without changing their eigenfrequencies. Unlike in linear cavities, the steady-state resonance

frequency in an ideal ring cavity does not depend on the position of the membrane, i.e.  $G \equiv 0$ . The standard theory for optomechanical damping would thus predict no damping at all. This is probably the reason why such ring cavities have not been discussed so far in the context of damping the motion of nanomechanical oscillators. [9, 10]. What has been studied extensively is the coupling of ring cavity modes to the mechanical motion of cold atom clouds consisting of many thousands of atomic oscillators with typically much smaller reflectivity than that of a dielectric membrane [11]. The rich physics of such coupled atom-photon-systems includes nonlinear dynamics, optical bistability, strong coupling, collective scattering, dynamic instabilities, and self-synchronization [12–18], topics which have all been discussed also in the context of cavity optomechanics [1]. Moreover, Gangl et al. predicted that cooling of particles can be even more efficient in ring cavities than in standing wave cavities [19]. It thus seems promising to start experiments with macroscopic oscillators inside mirror ring resonators.

As it turned out, the below presented observed damping rates cannot be understood without taking into account mirror back scattering. Residual imperfections of the dielectric mirror coatings can rescatter light between the two circulating modes of the ring resonator. One way to theoretically describe such back scattering is to introduce a fictitious partially reflecting intra cavity mirror that effectively captures the total scattering at all optical surfaces inside the resonator. Such a model, however, can easily be extended to describe two membranes in a ring resonator with the fictitious mirror now realized by the second membrane. With this in mind, we start Section II with deriving the equations for a ring cavity that contains two membranes. We calculate the steady state spectra and experimentally test them in air. Section III describes the main experiment and presents the observed mechanical damping rates in a single membrane resonator in vacuum. In the theoretical Section IV

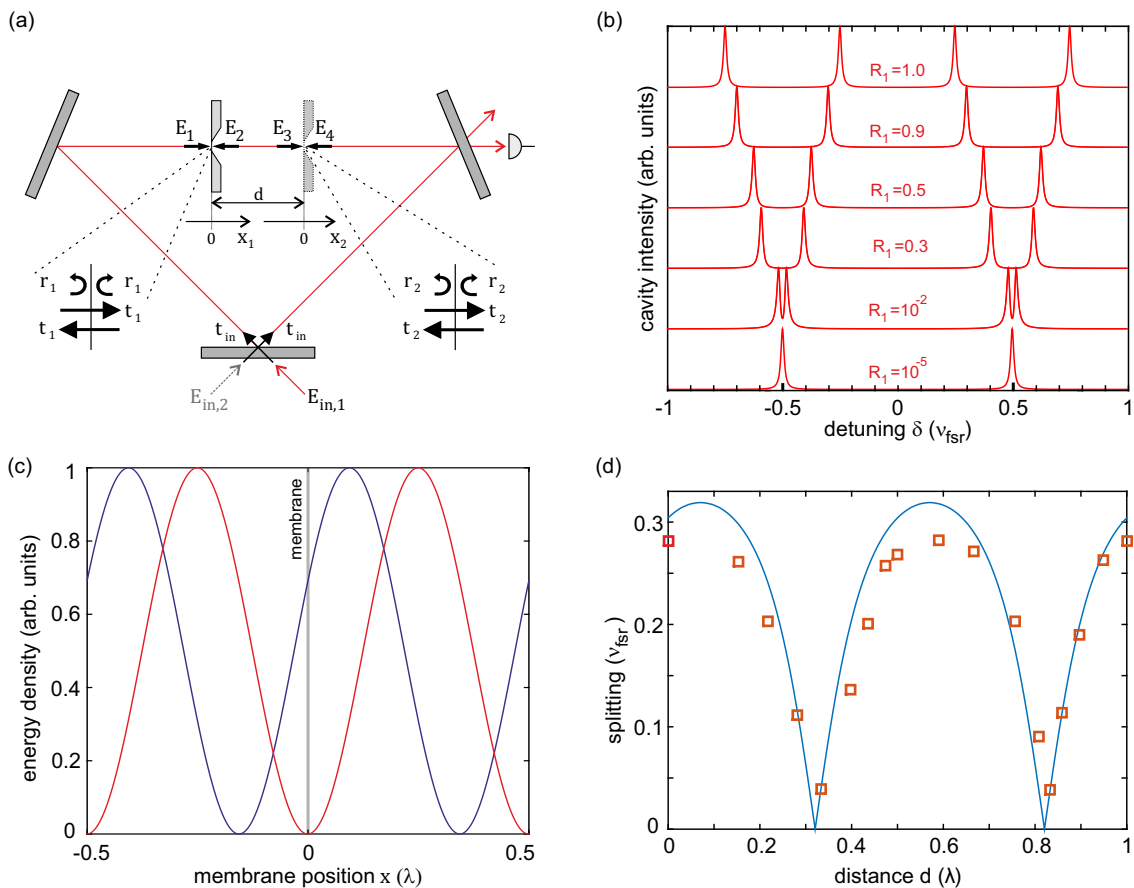


FIG. 1: (a) Sketch of the investigated setup. A ring resonator made from high quality dielectric mirrors contains two nano membranes with amplitude reflection  $r_i$ , transmission  $t_i$  and time dependent excursion  $x_i$ . The fields  $E_1$  to  $E_4$  are each evaluated at an infinitesimal displacement to the left resp. to the right of the membranes equilibrium position and are propagating clockwise resp. counter clockwise in the cavity. (b) Calculated spectra of a ring resonator that contains a single membrane with various reflection coefficient  $R_1 = |r_1|^2$ . The reflectivity of the second membrane is set to zero,  $R_2 = 0$ . The membrane couples the two circulating waves and lifts the mode degeneracy of an empty cavity. (c) Calculated energy density distribution of the standing light waves in the cavity for both eigenmodes with  $R_1 = 0.3$  and  $R_2 = 0$ . (d) Calculated mode splitting (blue curve) for a ring cavity with two membranes with various separations ( $R_1 = R_2 = 0.3$ ). Red squares denote the experimentally observed splitting with the cavity in air.

we write down the equations of motion and introduce a perturbation method to derive the optomechanical damping rates. We first apply the model to a single membrane in an ideal resonator. It can be solved fully analytically and is less involved than the full model for two membranes. In a second step, backscattering is included and the damping rate for the first membrane is calculated semi analytically with the second membrane held fixed in order to represent back scattering. Finally, the result is discussed and compared to damping in linear cavities. Section V concludes with an outlook to the physics in real ring resonators with two membranes.

## II. RESONATOR SPECTRA WITH ONE AND TWO MEMBRANES

The scenario discussed here is shown in Fig. 1 (a). A three mirror ring resonator contains two membranes with complex amplitude reflectivity  $r_1, r_2$  and transmittivity  $t_1, t_2$ . The membranes are at equilibrium positions  $d_1$  and  $d_2$  measured from the input coupling mirror clockwise and counter clockwise, respectively. They can oscillate around this position with a time dependent excursion  $x_i(t)$ . The cavity round-trip length  $l$  sets the value of the free spectral range  $\nu_{fsr} = c/l$  with  $c$  being the vacuum speed of light. The distance between the equilibrium positions of the membranes is  $d = l - d_1 - d_2$ . We describe the light inside the resonator in the basis of four traveling waves. Their steady state electric field amplitudes immediately left and right of the two membranes can be found by requiring self consistency after one round trip

time  $\tau = 1/\nu_{fsr}$ :

$$\begin{aligned}
E_1 &= t_2 E_3 r_c e^{-i\varphi_d} + r_2 E_4 r_c e^{-i\varphi_d - 2ikx_2} + t_{in} E_{in,1} e^{i\varphi_1} \\
E_2 &= r_2 E_3 e^{i\varphi_d + 2ikx_2} + t_2 E_4 e^{i\varphi_d} \\
E_3 &= r_1 E_2 e^{i\varphi_d - 2ikx_1} + t_1 E_1 e^{i\varphi_d} \\
E_4 &= t_1 E_2 r_c e^{-i\varphi_d} + r_1 E_1 r_c e^{-i\varphi_d + 2ikx_1} + t_{in} E_{in,2} e^{i\varphi_2}.
\end{aligned} \tag{1}$$

Here,  $r_c = r_l e^{ikl}$ ,  $\varphi_d = kd$ ,  $\varphi_1 = kd_1$ , and  $\varphi_2 = kd_2$ . The real valued parameter  $r_l$  describes the field amplitude reduction after one cavity round-trip due to transmission at the input coupling mirror. Uncontrolled losses due to scattering and absorption at the optical elements are also absorbed in an effective value for  $r_l$ . In equilibrium the excursions vanish,  $x_i(t) = 0$ . We solve Eq. (1) numerically for unidirectional pumping, i.e.  $E_{in,2} = 0$ , and plot the intra cavity laser intensities as a function of detuning. Spectra for a single membrane in an ideal resonator ( $R_2 = 0$ ) are shown in Fig. 1 (b). The coupling of the counterpropagating waves by the membrane leads to a splitting of the two eigenmodes that increases with  $R_1$ . In the limit of  $R_1 = 1$  the ring transforms into a standing wave cavity and the resulting equidistant spectrum is that of a linear cavity with a free spectral range which is half of that of the ring cavity. In the experimentally observed spectra (not shown here) the resonant intensity of the two eigenmodes is not exactly equal. This can be explained by the light intensity at the position of the membrane which is different for the two modes, see Fig. 1 (c). The amount of absorption inside the membrane is thus different. The plotted light distribution is particular for modeling the membrane as an infinitesimally thin dipole sheet which results in a specific phase of its complex reflectivity  $r_1$ . For comparison, we have also modeled the membrane as an extended layer with 50 nm thickness and calculated its total field reflectivity from the single boundary Fresnel reflectivities at both sides of the membrane. Using this more realistic model the position of the standing wave node is slightly shifted from the membrane position, but the qualitative behavior stays the same.

If the position of a single membrane is shifted, the resonance frequencies of the cavity modes do not change, i.e. for a single membrane in an ideal resonator  $G = 0$ . This is different if the cavity contains a second membrane. It generates its own standing wave in the cavity that adds to the standing wave generated by the first membrane. With increasing  $R_2$  the phase of the total standing wave decouples from the position of the first membrane and  $G$  can now differ from zero. The two membranes form an intra cavity Fabry-Perot etalon whose reflectivity depends on the membrane separation  $d$ . For destructive interference in reflection, the cavity spectrum is that of an ideal ring cavity without any internal reflector, i.e. the splitting observed in Fig. 1 (b) disappears. For constructive interference in reflection, the overall reflectivity of the intra cavity Fabry-Perot etalon becomes maximum and

the resulting splitting exceeds that of an ideal resonator with a single membrane. This behavior is captured in our model and we can compare the simulated splitting for  $R_1 = R_2 = 0.3$  to our experimental observation with two membranes in the ring cavity (Fig. 1 (d)). The experiment is performed in air and we vary the distance  $d$  with a piezo-transducer to which one of the membranes was attached. Note that the signal is periodic in  $\lambda/2$ . The plotted distance is thus defined only modulo half an optical wavelength  $\lambda$ . Simulations and measured data agree reasonably, with a global offset of the experimental value of  $d$  as only free parameter. From this offset all other distances are determined from the piezo voltage. We have also tested the model by recording the splitting caused by a single membrane, again with good agreement. Details about the resonator geometry are found in the next section.

### III. EXPERIMENTAL OBSERVATIONS

Experimentally it is difficult to keep a membrane perfectly aligned over a longer time in vacuum. In standing wave cavities a compact setup helps. For a ring resonator this approach has its limits and it is not yet clear how to solve the alignment problem with even two membranes in the resonator. We thus restrict ourselves to experiments with a single membrane. We glued the membrane (Norcada NX5100A, low-stress,  $1 \text{ mm}^2 \times 50 \text{ nm}$ ) on a piezo-transducer and positioned it in the mode volume of the ring cavity with round-trip length  $l = 8.5 \text{ cm}$ . The angle of the membrane with respect to the cavity axis is adjusted for normal incidence by means of a compact and stable precision mirror mount. The finesse of the cavity including the membrane has been determined to be  $F = 520$  by modulating the phase of the laser beam with a frequency of 20 MHz and using the resulting side bands as frequency markers for measuring the linewidth of the resonator. The cavity mirrors are dielectric "super mirrors" with specified scattering losses below 5 ppm. These extreme values are only reached in a clean room environment and may be somewhat higher in our experiment. The transmission of the input coupler is  $T_{in} = |t_{in}|^2 = 6.04 \times 10^{-3}$ . The cavity including the nanomembrane is placed in a vacuum chamber at a pressure of  $p = 2 \times 10^{-8} \text{ mbar}$  and is single sided pumped with  $P_{in} = 10 \text{ mW}$  by a standard grating stabilized diode laser at a wavelength near 780 nm. The laser frequency  $\nu$  is electronically stabilized to the resonance frequency of the cavity  $\nu_c$  with variable detuning  $\Delta = \nu_c - \nu$ . Once the laser frequency is locked, the membrane is mechanically excited with a piezo-transducer that is harmonically driven at the resonance frequency of the membrane  $\Omega_m \simeq 2\pi \times 130 \text{ kHz}$ . The oscillation of the membrane is detected by overlapping the two counterpropagating modes on a beam splitter outside the cavity. Due to the motion of the membrane the electric fields of the two modes are phase-modulated with the membrane

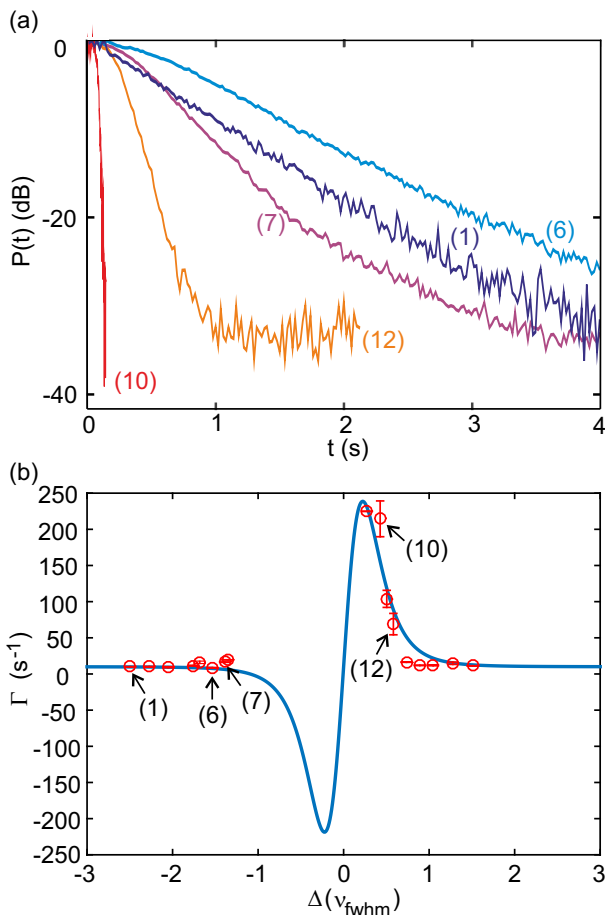


FIG. 2: (a) Ring-down measurements of membrane oscillation. For clarity, only some of the curves are plotted, the number indicating the corresponding data point in the part (b) of the figure. (b) Experimentally determined damping rates. The error bars indicate the statistical error by evaluating several curves with identical detuning. The solid line is plotted solely for guiding the eye and illustrating the dispersive lineshape of the data points.

frequency  $\Omega_m$ . The detected beat signal at  $\Omega_m$  is analyzed with a spectrum analyzer in zero-span mode. The measured power signal  $P(t)$  is thus proportional to the quadratic displacement  $x^2(t)$  of the membrane. After exciting the membrane, we quickly switch-off the piezo drive and measure the decrease of  $P(t)$  in a ring-down experiment, see Fig. 2 (a). We determine the damping rate  $\Gamma$  by an exponential fit  $P(t) \propto \exp(-2\Gamma t)$ . The result is plotted in Fig. 2 (b). No data could be taken close to resonance for negative detuning because of strong self-sustained oscillations. For positive detuning the maximum damping rate amounts to about  $250 \text{ s}^{-1}$ . The intrinsic damping of the membrane was determined at large detuning to be  $10 \text{ s}^{-1}$ .

#### IV. OPTOMECHANICAL DAMPING OF A SINGLE MEMBRANE IN A RING CAVITY

In an ideal ring resonator without mirror back scattering a single membrane is the only element that couples the two counter propagating traveling wave modes. Therefore, a two mode model with amplitudes  $E_1$  and  $E_2$  is sufficient and the modes with amplitudes  $E_3$  and  $E_4$  can be dropped. Similar to the equations (1) we look at the amplitudes after one round trip time  $\tau = 1/\nu_{fsr}$ .

$$\begin{aligned} E_1(t + \tau) &= tr_c E_1(t) + r_c r e^{-2ikx} E_2(t) + t_{in} E_{in,1} e^{i\varphi_1} \\ E_2(t + \tau) &= tr_c E_2(t) + r_c r e^{2ikx} E_1(t) . \end{aligned} \quad (2)$$

For simplicity, we drop the indices in  $r_1$ ,  $t_1$ , and  $x_1$  for a single membrane. The equations of motion are obtained by first order Taylor-expansion  $E_i(t + \tau) \simeq E_i(t) + \tau \dot{E}_i(t)$ . The result can be expressed as

$$\frac{d}{dt} \vec{E} = M(t) \vec{E} + \vec{\eta}, \quad (3)$$

with matrix

$$\begin{aligned} M &= \nu_{fsr} \begin{pmatrix} A & B \\ C & A \end{pmatrix}, \\ A &:= tr_c - 1, \quad B := r_c r e^{-i2kx}, \quad C := r_c r e^{i2kx}, \end{aligned} \quad (4)$$

and field pump rate

$$\vec{\eta} = \begin{pmatrix} \eta \\ 0 \end{pmatrix}, \quad \eta := \sqrt{\frac{T_{in} P_{in}}{\hbar k c}} \nu_{fsr}. \quad (5)$$

The matrix  $M(t)$  contains the motion of the membrane  $x(t)$  which varies slowly in time as compared to the time scale of the cavity field dynamics. We thus can solve equation (3) with the perturbation ansatz

$$\vec{E} = \vec{E}_a(t) + \vec{\delta}(t), \quad (6)$$

with  $\vec{\delta}(t)$  being the non adiabatic correction to the instantaneous adiabatic solution  $\vec{E}_a(t) = -M(t)^{-1} \vec{\eta}$ . Inserting the ansatz (6) into (3) provides a differential equation for  $\vec{\delta}(t)$ .

$$\frac{d}{dt} \vec{\delta} = M(t) \vec{\delta} + \frac{d}{dt} \left( M(t)^{-1} \vec{\eta} \right). \quad (7)$$

We approximately solve this equation by assuming the nonadiabatic correction to be always in equilibrium,  $d\vec{\delta}/dt = 0$ . This results in

$$\vec{\delta}(t) = -M(t)^{-1} \frac{d}{dt} \left( M(t)^{-1} \vec{\eta} \right). \quad (8)$$

Inserting the matrix  $M$  from Eq. (4) into Eq. (8) the approximate solution of the problem (3) can be written analytically as

$$\begin{aligned}\vec{E}_a &= -\frac{\eta\nu_{fsr}}{\det(M)} \begin{pmatrix} A \\ -C \end{pmatrix}, \\ \vec{\delta} &= 2ik\dot{x} \frac{\eta\nu_{fsr}^2}{(\det(M))^2} C \begin{pmatrix} -B \\ A \end{pmatrix},\end{aligned}\quad (9)$$

More formally speaking, this procedure is equivalent to replacing the total differential  $\frac{d}{dt}$  by  $\frac{\partial}{\partial t} + v\frac{\partial}{\partial x}$  and expanding the fields in powers of the membrane velocity  $v = \dot{x}$ ,  $E_{\pm} = E_{\pm}^{(0)} + vE_{\pm}^{(1)} + \mathcal{O}(v^2)$  [23]. Keeping only first order terms is a good approximation if the energy decay rate of the cavity  $\kappa$  is much larger than the oscillation frequency of the membrane  $\Omega_m$  ("Doppler limit"). For our experiment this is well fulfilled ( $\Omega_m = 2\pi \times 130$  kHz,  $\kappa = 2\pi \times 3.6$  MHz).

### A. Forces on the membrane

The forces on the membrane are derived from momentum conservation for the fields  $\vec{E}_1$  and  $\vec{E}_2$  and the membrane. Analogous to optical forces on cold atoms, the forces can be separated into reflection and dipole force

$$\begin{aligned}F_{ref} &= 2\hbar k\nu_{fsr} \cdot |r|^2 \left( |E_1|^2 - |E_2|^2 \right) \\ F_{dip} &= 2i\hbar k\nu_{fsr} \text{Im}(r) \left( E_1 E_2^* e^{2ikx} - E_1^* E_2 e^{-2ikx} \right).\end{aligned}\quad (10)$$

The radiation pressure force due to photon absorption in the membrane is very small and can be neglected. By inserting the ansatz (6) into (10) and in the approximation of small oscillation amplitude,  $x \ll \lambda$ , the viscous parts of the forces proportional to  $\delta \propto \dot{x}$  take the form

$$\begin{aligned}F_{ref,\dot{x}} &= 4\hbar k\nu_{fsr} \cdot |r|^2 \text{Re}(E_{a,1}\delta_1^* - E_{a,2}\delta_2^*), \\ F_{dip,\dot{x}} &= 4i\hbar k\nu_{fsr} \text{Im}(r) \text{Im}(E_{a,1}\delta_2^* + E_{a,2}\delta_1).\end{aligned}\quad (11)$$

The total damping force is related to the optomechanical damping rate by  $F = F_{ref,\dot{x}} + F_{dip,\dot{x}} = m_{eff}\Gamma_{opt}\dot{x}$  resulting in

$$\begin{aligned}\Gamma_{opt} &= \Gamma_0 \cdot K_1 \cdot K_2, \\ \Gamma_0 &:= \frac{T_{in}P_{in}}{m_{eff}c^2} kl, \\ K_1 &:= \frac{8}{|p^2 - q^2|^4}, \\ K_2 &:= \text{Re}(q^*(p^2 - q^2)) \times \\ &\quad \times \left( 2|r|^2 \text{Im}(pq^*) - \text{Im}(r) \left( |p|^2 - |q|^2 \right) \right), \\ p &:= tr_c - 1 \quad q := rr_c.\end{aligned}\quad (12)$$

We are interested in the damping rates near the optical resonances of the cavity. The frequency dependence is described by the complex round trip reflectivity  $r_c = r_l e^{ikl}$  which contains the phase  $\phi = kl$  that the light field accumulates during one round-trip. By analyzing the resonance denominator of  $K_1$  one finds that there are two resonances at  $\phi = \phi_{\pm}$  with  $e^{i\phi_{\pm}} = r \pm t$ . We expand  $\Gamma_{opt}(\phi)$  around the resonance  $\phi_+$  by setting  $\cos(\phi_+ - \phi) \approx 1 - \frac{1}{2}(\phi_+ - \phi)^2$ . The frequency detuning  $\Delta$  and the cavity energy decay rate  $\kappa$  can be expressed by  $\Delta = \nu_{fsr}(\phi_+ - \phi)$  and  $\kappa = 2\nu_{fsr}(1 - r_l)$ . We also make the standard approximation  $1 - r_l^2 = (1 + r_l)(1 - r_l) \approx 2(1 - r_l) = \frac{\kappa}{\nu_{fsr}} = \frac{\pi}{F}$  which is valid for small round-trip losses, i.e.  $r_l \approx 1$ . Finally one arrives at an analytic expression for the optomechanical damping rate of a single membrane in an ideal ring resonator:

$$\Gamma_{opt} = \frac{1}{4}\Gamma_0 \cdot \nu_{fsr}^2 \frac{-4\Delta\kappa}{(\kappa^2/4 + \Delta^2)^2} \quad (13)$$

The extreme values

$$\Gamma_{\max} = \mp \frac{3\sqrt{3}}{8}\Gamma_0 \cdot \left(\frac{F}{\pi}\right)^2 \quad (14)$$

are obtained for the detuning  $\Delta = \pm \frac{1}{6}\sqrt{3}\kappa$ . With the numbers of our experiment  $m_{eff} = 3.88 \times 10^{-11}$  kg,  $\nu_{fsr} = c/l = 3.75$  GHz,  $F = 520$ ,  $T_{in} = t_{in}^2 = 6.04 \times 10^{-3}$ , and  $P_{in} = 10$  mW the maximum damping rate amounts to  $\Gamma_{\max} = -0.2$  s $^{-1}$ . This value is approximately 3 orders of magnitude smaller than what we observe experimentally. Thus, the damping mechanism analyzed so far cannot be the main reason for our observation. Good agreement can be reached, however, if mirror back scattering is included.

### B. Mirror back scattering

Unavoidable scattering at imperfections of a mirror surface may couple the circulating modes of a ring cavity [24]. In our experiment we have thus used best available mirrors and the finesse of the empty ring resonator can reach values of up to 150000. Still, back scattering is clearly detectable and must be taken into account. A complete description is quite involved since every optical surface in the cavity may contribute. Depending on the position of these surfaces the various contributions interfere with different phases. These interferences are different for each longitudinal mode. Furthermore, the Purcell effect enhances scattering into cavity modes of high finesse. We circumvent these details and assume that all scatterers together act like an additional reflecting element inside the cavity with an effective complex field reflectivity and transmittivity  $r_2$  and  $t_2$ . The system is then equivalent to the two membrane system shown in Fig. 1(a) and the equations (1) can be used as a starting point for deriving the equations of motion. The procedure is the same as shown in detail in the preceding

section for a single membrane, with the difference that four light fields are involved, and no practical analytical solution can be found. In particular, Eq. (3) is still valid

$$M := \begin{pmatrix} -\frac{1}{\tau_r} & 0 & \frac{1}{\tau_r} t_2 r_{11} e^{ikl-i\varphi_d} & \frac{1}{\tau_r} r_2 r_{11} e^{ikl-i\varphi_d-2ikx_2} \\ 0 & -\frac{1}{\tau_d} & \frac{1}{\tau_d} r_2 r_{12} e^{i\varphi_d+2ikx_2} & \frac{1}{\tau_d} t_2 r_{12} e^{i\varphi_d} \\ \frac{1}{\tau_d} t_1 r_{12} e^{i\varphi_d} & \frac{1}{\tau_d} r_1 r_{12} e^{i\varphi_d-2ikx_1} & -\frac{1}{\tau_d} & 0 \\ \frac{1}{\tau_r} r_1 r_{11} e^{ikl-i\varphi_d+2ikx_1} & \frac{1}{\tau_r} t_1 r_{11} e^{ikl-i\varphi_d} & 0 & -\frac{1}{\tau_r} \end{pmatrix}, \vec{\eta} = \begin{pmatrix} \eta \\ 0 \\ 0 \\ 0 \end{pmatrix}, \quad (15)$$

where we have introduced two different delay times  $\tau_d := \frac{d}{c}$  and  $\tau_r := \frac{l-d}{c}$ . The losses are distributed within the cavity:  $r_{l1}$  describes the losses along the path from one membrane to the other membrane via the input coupler and  $r_{l2}$  describes the losses along the direct path between the membrane. The first membrane may oscillate while the second membrane is held fixed at  $x_2 = 0$ . The stationary solution for the nonadiabatic correction (8) now reads

$$\vec{\delta}(t) = 2ik\dot{x}_1 (M^{-1}(t))^2 D M^{-1} \vec{\eta}, \quad (16)$$

with

$$D = \begin{pmatrix} 0 & 0 & 0 & 0 \\ 0 & 0 & 0 & 0 \\ 0 & -\frac{1}{\tau_d} r_1 r_{12} e^{i\varphi_d} & 0 & 0 \\ \frac{1}{\tau_r} r_1 r_{11} e^{ikl-i\varphi_d} & 0 & 0 & 0 \end{pmatrix}. \quad (17)$$

The solution for the instantaneous field  $\vec{E}_a$  and the correction  $\vec{\delta}$  can easily be calculated numerically together with the forces according to Eq. (11). The calculations are done with a separation between the membrane and the reflector set to  $d = l/2$ . The losses are equally distributed,  $r_{l1} = r_{l2}$  with total losses according to a Finesse of 520. The red line in Fig. 3 presents the resulting maximum damping rates for various reflectivities  $R_2 = |r_2|^2$ . For decreasing  $R_2$ , mirror backscattering becomes less and less important. The damping rate levels off and approaches the analytical solution for an ideal resonator with a single membrane, (Eq. (14), lower dashed line). In the opposite limit of  $R_2 = 1$  the ring cavity is equivalent to the standard geometry of a linear cavity with a membrane between the mirrors (MIM). The damping rate of this limit is already reached for values of  $R_2 > R_1 = 0.3$ , above which the standing wave inside the resonator is locked to the position of the second membrane.

For MIM-systems an analytic expression for the damping rate in the Doppler limit ( $\kappa \gg \Omega_m$ ) is given in [1]

$$\Gamma_{MIM} = -\frac{1}{2} G^2 \frac{P_{in}}{m_{eff} \omega} \cdot T_{in} \nu_{fsr} \cdot \frac{4\kappa\Delta}{(\kappa^2/4 + \Delta^2)^3}. \quad (18)$$

with the matrix  $M$  and the pumping vector  $\vec{\eta}$  now being four-dimensional. The matrix  $M$  reads

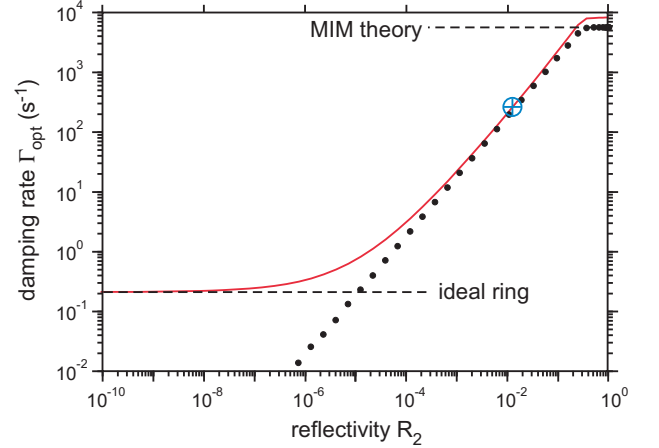


FIG. 3: Optomechanical damping rate of a membrane inside a ring cavity as function of the reflectivity  $R_2$  of an additional reflector. The separation between the membrane and the reflector is set to  $d = l/2$  and the losses are equally distributed,  $r_{l1} = r_{l2}$  with the total losses according to a Finesse of 520. In the standing wave limit,  $R_2 = 1$ , this choice allows a direct comparison with the standard description of a MIM-System according to Eq. (20) (upper dashed line). The lower dashed line indicates the result for a single membrane in an ideal ring cavity, Eq. (14). The black dots are the result of the expression Eq. (18) by inserting  $G$  as determined from calculated ring cavity spectra. The blue cross corresponds to the highest experimentally observed damping rate.

The coefficient  $G = d\omega_c/dx_1$  is the derivative of the cavity resonance frequency

$$\omega_c = \frac{c}{l_{MIM}} \arccos \left( \sqrt{R} \cos(2k(x_0 + x_1)) \right), \quad (19)$$

with respect to the excursion  $x_1$  of the membrane at the steady state position  $x_0$  [6].  $R = |r|^2$  is the reflectivity of the membrane and  $l_{MIM}$  is the mirror separation of the standing wave resonator. Maximum damping  $\Gamma_{MIM,max}$  is obtained for  $2kx_0 = \frac{\pi}{2}$  and  $\Delta = \pm \frac{\sqrt{5}}{10} \kappa$ . Using the

same notation as in Eq. (14) one obtains

$$\Gamma_{MIM,\max} = -\frac{16 \cdot 200}{27} \sqrt{5} R_1 \Gamma_0 \left( \frac{F}{2\pi} \right)^4. \quad (20)$$

Note that for  $R_2 = 1$  the resulting standing wave cavity has a mirror separation of  $2l$ . With the parameters of our experiment the maximum damping rate amounts to  $\Gamma_{MIM,\max} = 5.6 \times 10^3 \text{ s}^{-1}$ , (upper dashed line in Fig. 3). This is slightly below the value obtained from our four mode model. This discrepancy is to be expected since Eq. (18) is derived from a single mode model that does not take into account the nonadiabatic correction to the mode function during the oscillation of the membrane. Instead, the instantaneous steady state mode is used and the model explains damping by the nonadiabatic correction to the mode occupation alone. A full two mode model is described in ref. [25] but an analytic expression is not reported.

Our observed damping rate of  $\Gamma \sim 250 \text{ s}^{-1}$  (blue cross in Fig. 3) can now be explained if we assume an realistic value for the effective mirror back scattering of  $R_2 \sim 1\%$ .

### C. Phase coupling vs. frequency coupling

The damping mechanism in an ideal ring resonator in the limit of  $R_2 \rightarrow 0$  is fundamentally different from that usually discussed in optomechanics. In the latter, a displacement of the membrane detunes the cavity resonance relative to the frequency of the incoupled light which changes the steady state light power in the cavity ("frequency coupling"). In contrast, a membrane displacement in an ideal ring cavity has no effect on the cavity resonance frequency and the steady state light power does not change. In an ideal ring resonator it's the steady state position of the standing wave inside the resonator that is shifted by the membrane ("phase coupling"). In a real ring resonator with mirror back scattering, both effects play a role. In order to distinguish the contributions of frequency and phase coupling, we calculate the steady state resonance frequency for various membrane positions  $x_0$  and derive the frequency shift per membrane excursion  $G = d\omega_c/dx_1$  for each  $x_0$ . Similar as in linear cavities one obtains a periodic function  $G(x_0)$ . We extract the maximum value  $G_{\max} = \max(G(x_0))$  and use Eq. (18) to calculate the optomechanical damping rate. Its dependency on the reflectivity  $R_2$  is shown in Fig. 3 as black dots. In

the linear cavity limit ( $R_2 = 1$ ), there is exact agreement with the analytical single mode MIM-model (upper dashed line), as expected. However, in the ring cavity limit,  $R_2 \rightarrow 0$ , the damping rate tends to zero due to a vanishing value of  $G$ . This is in contrast with the exact solution (red line) which levels off for values of  $R_2 \lesssim 10^{-5}$ . It is quite surprising that frequency coupling dominates phase coupling already at such minute values for  $R_2$ . Pure phase coupling thus seems hard to achieve experimentally.

## V. SUMMARY AND OUTLOOK

We have analyzed the damping of a nanomembrane inside an optical ring cavity and found a novel optical damping mechanism that is based on the coupling of the membrane to the phase of the light field. Furthermore, we have identified the reflectivity  $R_2$  of a second reflector as crucial parameter for modeling our experimentally observed damping rates. This second reflector is used to describe mirror back scattering but it also may represent a second membrane in the cavity. Since pure phase coupled damping ( $R_2 = 0$ ) is small and hard to observe it is probably more interesting for future work to investigate ring resonators with two or more mechanical oscillators. We have analyzed synchronization by applying the above described perturbation method to a system of two moving membranes. For the parameters of our experiment we find that the relative motion is damped with a high rate of several  $10^4 \text{ s}^{-1}$  which is comparable to the values obtained for standard MIM-systems. This indicates that optical coupling of the oscillators via the cavity fields leads to efficient phase synchronization. Ring cavities thus seem to provide a promising playground for studying light mediated coupling of two or more mechanical oscillators. If applied to oscillators in their quantum ground state, such long-range coupling may allow for the construction of entangled states and quantum state transfer between distant oscillators.

S. Slama is indebted to the Baden-Württemberg Stiftung for the financial support of this research project by the Eliteprogramm for Postdocs. A. Yilmaz is funded by Deutsche Telekom Stiftung. We acknowledge helpful discussion with Florian Marquardt. Competing financial interests do not exist.

- 
- [1] Markus Aspelmeyer, Tobias J. Kippenberg, and Florian Marquardt. Cavity Optomechanics. *Rev. Mod. Phys.* **86**, 1391 (2014)
- [2] J.D. Teufel, T. Donner, D. Li, J. W. Harlow, M. S. Allman, K. Cicak, A. J. Sirois, J.D. Whittaker, K.W. Lehnert, and R.W. Simmonds. Sideband cooling of microme-

chanical motion to the quantum ground state. *Nature (London)* **475**, 359 (2011)

- [3] Jasper Chan, T.P. Mayer Alegre, Amir H. Safavi-Naeini, Jeff T. Hill, Alex Krause, Simon Gröblacher, Markus Aspelmeyer, and Oskar Painter. Laser cooling of a nanomechanical oscillator into its quantum ground state. *Nature*

- (London) **478**, 89 (2011)
- [4] K. Usami, A. Naesby, T. Bagci, B. Melholdt Nielsen, J. Liu, S. Stobbe, P. Lodahl, and E.S. Polzik. Optical cavity cooling of mechanical modes of a semiconductor nanomembrane. *Nature Phys.* **8**, 168 (2012)
- [5] C. Metzger, M. Ludwig, C. Neuenhalm, A. Ortlieb, I. Favero, K. Karrai, and F. Marquardt. Self-induced Oscillations in an Optomechanical System Driven by Bolometric Backaction. *Phys.Rev.Lett.* **101**, 133903 (2008)
- [6] J.D. Thompson, B.M. Zwickl, A.M. Jayich, Florian Marquardt, S.M. Girvin, and J.G.E. Harris. Strong dispersive coupling of a high-finesse cavity to a micromechanical membrane. *Nature* **452**, 72 (2008)
- [7] D.J. Wilson, C.A. Regal, S.B. Papp, and H.J. Kimble. Cavity Optomechanics with Stoichiometric SiN Films. *Phys.Rev.Lett.* **103**, 207204 (2009)
- [8] G. Anetsberger, O. Arcizet, Q.P. Unterreithmeier, R. Rivière, A. Schliesser, E. M. Weig, J. P. Kotthaus and T. J. Kippenberg. Near-field cavity optomechanics with nanomechanical oscillators. *Nature Phys.* **5**, 909 (2009)
- [9] Please note that membranes in ring-like Michelson-Sagnac interferometers like in [10] are equivalent to the membrane-in-the-middle setup.
- [10] A. Sawadsky, H. Kaufer, R. M. Nia, S. P. Tarabrin, F. Y. Khalili, K. Hammerer, and R. Schnabel. Observation of Generalized Optomechanical Coupling and Cooling on Cavity Resonance. *Phys.Rev.Lett.* **114**, 043601 (2015)
- [11] Helmut Ritsch, Peter Domokos, Ferdinand Brennecke, and Tilman Esslinger. Cold atoms in cavity-generated dynamical optical potentials. *Rev.Mod.Phys.* **85**, 553 (2013)
- [12] B. Nagorny, Th. Elsässer, and A. Hemmerich. Collective Atomic Motion in an Optical Lattice Formed Inside a High Finesse Cavity. *Phys.Rev.Lett* **91**, 153003 (2003)
- [13] Th. Elsässer, B. Nagorny, and A. Hemmerich. Optical bistability and collective behavior of atoms trapped in a high-Q ring cavity. *Phys.Rev.A* **69**, 033403 (2004)
- [14] Julian Klinner, Malik Lindholdt, Boris Nagorny, and Andreas Hemmerich. Normal Mode Splitting and Mechanical Effects of an Optical Lattice in a Ring Cavity. *Phys.Rev.Lett.* **96**, 023002 (2006)
- [15] D. Kruse, C. von Cube, C. Zimmermann, and Ph.W. Courteille. Observation of Lasing Mediated by Collective Atomic Recoil. *Phys.Rev.Lett.* **91**, 183601 (2003)
- [16] S. Slama, S. Bux, G. Krenz, C. Zimmermann, and Ph. Courteille. Superradiant Rayleigh Scattering and Collective Atomic Recoil Lasing in a Ring Cavity. *Phys.Rev.Lett.* **98**, 053603 (2007)
- [17] D. Schmidt, H. Tomczyk, S. Slama, and C. Zimmermann. Dynamical Instability of a Bose-Einstein Condensate in an Optical Ring Resonator. *Phys.Rev.Lett.* **112**, 115302 (2014)
- [18] C. von Cube, S. Slama, D. Kruse, C. Zimmermann, Ph. Courteille, G. Robb, N. Piovella, and R. Bonifacio. Self-Synchronization and Dissipation-Induced Threshold in Collective Atomic Recoil Lasing. *Phys.Rev.Lett.* **93**, 083601 (2004)
- [19] Markus Gangl, Peter Horak, and Helmut Ritsch. Cooling neutral particles in multimode cavities without spontaneous emission. *J.Mod.Opt.* **47**, 2741 (2000)
- [20] K. Hammerer, M. Aspelmeyer, E. S. Polzik, and P. Zoller. Establishing Einstein-Poldosky-Rosen Channels between Nanomechanics and Atomic Ensembles. *Phys.Rev.Lett.* **102**, 020501 (2009)
- [21] A. Jöckel, A. Faber, T. Kampschulte, M. Korppi, M.T. Rakher, and Ph. Treutlein. Sympathetic cooling of a membrane in a hybrid mechanical-atomic system. *Nature Nanotech.* **10**, 55-59 (2015)
- [22] Eugene S. Polzik and Jun Ye. Entanglement and spin-squeezing in a network of optical lattice clocks. *Phys. Rev. A* **93**, 021404(R) (2016)
- [23] P. Domokos and H. Ritsch. Mechanical effects of light in optical resonators. *J.Opt.Soc.Am. B* **20**, 1098 (2003), and M. Herzog, *Forces on mobile optical elements in a ring cavity*. Diploma thesis, University of Potsdam (2008)
- [24] G. Krenz, S. Bux, S. Slama, C. Zimmermann, and Ph.W. Courteille, Controlling mode locking in optical ring cavities. *Appl. Phys. B* **87**, 643 (2007)
- [25] A. M. Jayich, J. C. Sankey, B. M. Zwickl, C. Yang, J. D. Thompson, S. M. Girvin, A. A. Clerk, F. Marquardt, and J. G. E. Harris, Dispersive optomechanics: a membrane inside a cavity. *New Journal of Physics*, **10**, 095008 (2008)